

# Phonons as waves: the semiclassical theory of electrical resistivity

Eric J. Heller,<sup>1,2</sup> Alvar Daza,<sup>1,3</sup> Donghwan Kim,<sup>2</sup> and Kobra N. Avanaki<sup>1,2</sup>

<sup>1</sup>*Department of Physics, Harvard University, Cambridge, MA 02138*

<sup>2</sup>*Department of Chemistry and Chemical Biology, Harvard University, Cambridge, MA 02138*

<sup>3</sup>*Nonlinear Dynamics, Chaos and Complex Systems Group, Departamento de Física, Universidad Rey Juan Carlos, Tulipán s/n, 28933 Móstoles, Madrid, Spain*

(Dated: October 6, 2020)

Using a coherent state representation of phonons, thus treating them as waves rather than as countable particles or quanta, metallic conduction electrons are found to be traversing a confused, dynamic, blackbody-like sea of forces. Electrons can be treated semiclassically, buffeted by unceasing quasi-elastic collisions with the deformation potential, limiting mobility. This leads to a nonperturbative paradigm, consistent with existing theory in the perturbative limit. Explaining the normal resistivity of pure metals from 0 Kelvin to melting in a new language. It extends well beyond perturbation theory, both in intuitive insight and computational power. Using a coherent state representation brings the lattice alive, giving every atom a nonequilibrium position and momentum. The phonon sea grows in wave height as temperature is increased. Below the Bloch-Grüneisen transition, raising the temperature adds ever shorter wavelength components to the seas, causing a fast rise in resistivity. Above the Bloch-Grüneisen temperature, it rises as  $T$  in the weak field limit.

Electron-phonon interactions are fundamental to electronic devices, power transmission, superconductivity, and much more. There is scarcely a topic more central in the many excellent condensed matter physics texts or in much of a large condensed matter literature. A wavepacket or coherent state picture is always available and equivalent to number state representations. Here we develop a “phonon as wave” paradigm and find that a new narrative for electron-phonon interactions emerges.

The traditional one-phonon perturbation theory approach to electron-phonon interactions traces back to the 1950 paper of Bardeen and Shockley [1] who introduced the notion of a deformation potential resulting from phonon induced lattice strain. Using a quantized phonon eigenstate basis for the lattice, the deformation potential has been successfully introduced as a perturbation, and used as input to Boltzmann transport theory. This leads to the Bloch-Grüneisen formula for resistivity (see Ziman [2] and Das Sarma [3] for a clear exposition). Phonons are treated in particle-like fashion, counted individually, with discrete momentum changes delivered inelastically.

On the other hand, using a coherent state representation is especially appropriate for a crystal lattice. This representation animates the lattice motion, resulting in time dependent deformations inducing forces on the electrons that are in a semiclassical regime with respect to the Fermi wavelength. This allows use of *nonperturbative* semiclassical trajectory based methods, just as external electromagnetic fields are routinely treated (figure 1)[4]. Another antecedent of the present work is found in the treatment of ultrasound attenuation in pure metals[5, 6], where it is compelling to treat the acoustic ultrasound phonon as a wave.

Electron paths become a branched flow, deflected by a quasirandom phonon deformation landscape. Metallic

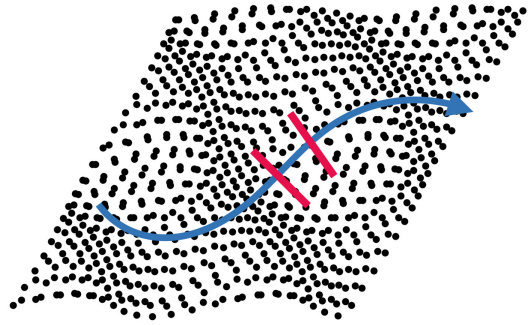


FIG. 1. The nuclear positions specified by a coherent state of a lattice are seen to be a wave of acoustic mode compressions and rarefactions, in this schematic. The deBroglie wavelength of the electron (red hatches) is shorter than the phonon wavelengths, justifying a semiclassical treatment of the electron subject to forces induced by modulation of local band energies.

resistivity is another example of branched flow systems, which include light propagating in dynamic soap bubble films [7], imaging electron branched flow in a two dimensional semiconductor [8], and tsunami waves [9].

Lattice deformations come alive if we replace lattice mode eigenstates with time dependent coherent states. There is an exact coherent state thermal ensemble for doing this [10]. Any phonon coherent state of all the modes implies specific dynamic lattice positions, which move classically (see figure 1). Schrödinger knew that the mean position and momentum of the atoms evolves classically in a harmonic oscillator [11, 12].

*Semiclassical deformation model.* Consider a uniform metal crystal at 0 Kelvin. For given band structure  $E(\vec{k})$ , the electron group velocity is  $d\vec{r}/dt = \partial E(\vec{k})/\partial(\hbar\vec{k})$ ;  $\vec{r}$

and  $\hbar\vec{k}$  are single electron position and momentum, respectively. If there are externally applied electric and magnetic fields  $\vec{\mathcal{E}}$  and  $\vec{\mathcal{B}}$ , the traditional phenomenological semiclassical model gives  $d(\hbar\vec{k})/dt = -e\vec{\mathcal{E}}(\vec{r}, t) - \frac{e}{c}\vec{r} \times \vec{\mathcal{B}}(\vec{r}, t)$ ;  $c$  is the speed of light [4, 13].

A crucial observation is that electrons are in a semiclassical regime with respect to the deformation potential, having short Fermi level electron wavelengths compared to the length scale of the deformation field. This supports the idea that the deformation potential can be considered a classical field acting on the electrons, just as external fields are treated.

If interference effects become important, the full quantum version of the single electron dynamics is an option, using for example the semiclassical Van Vleck-Morette-Gutzwiller Green function (the stationary phase version of the Feynman path integral). This parallels a program by Lifshitz and Koesvich [14] for *external* fields.

*The deformation potential.* The ingredients for constructing a deformation potential begin with phonon induced lattice displacements. The important parameter is changes in atom-atom distances, *i.e.*, the strain field [15]; rigid movement of groups of atoms are of little consequence.

The deformation potential at temperature  $T$  becomes a time dependent sum over all longitudinal acoustic phonon modes of all propagation directions with a weighting given by (the square root of) Bose occupations,

$$V_D(\vec{r}, t) = \frac{\mathbb{E}_d}{v_s} \sum_{\substack{\vec{q} \\ |\vec{q}| < q_{max}}} \sqrt{\frac{2\hbar\omega_{\vec{q}} \cos(\vec{q} \cdot \vec{r} - \omega_{\vec{q}}t + \phi_{\vec{q}})}{\rho_m V \sqrt{\exp(\hbar\omega_{\vec{q}}/k_B T) - 1}}} \quad (1)$$

where  $\vec{q}$  is a phonon wavevector,  $\phi_{\vec{q}}$  is an arbitrary phase shift of each mode,  $v_s$  is the longitudinal acoustic sound speed and  $\omega_{\vec{q}} = v_s|\vec{q}|$ ,  $\mathbb{E}_d$  is the deformation potential constant that varies from several eV to tens of eV,  $\rho_m$  and  $V$  are the mass density and the volume (or area in case of 2D) of metals or semimetals, respectively,  $\hbar$  is the reduced Planck constant, and  $k_B$  is the Boltzmann constant. Since the sum over the phonons is cut off at some  $q_{max}$ , the deformation potential is a modified blackbody field at higher temperatures.

The phonon wavenumber is bounded by either the Debye wavenumber  $q_D$  or twice the Fermi wavenumber  $2k_F$ , *i.e.*,  $q_{max} = \min\{q_D, 2k_F\}$ . Undulations in the deformation potential shorter than (the half of) Fermi wavelengths (or in momentum space,  $q > 2k_F$ ) have little refractive influence on the electrons at the Fermi level, as if they were not present. This is a well known ballistic transparency effect for small scale fluctuations of a medium that are uniform when averaged over a wavelength or so [16], familiar for visible light in clear glass for example.

Metals normally have large Fermi surfaces, so  $q_D < 2k_F$  and the cutoff occurs at the Debye wavenumber,  $q_{max} = q_D$ , while for semimetals Fermi surfaces are small, thus  $q_D > 2k_F$  and the cutoff occurs at the (twice of the)

Fermi wavenumber,  $q_{max} = 2k_F$  [17]. Therefore, the critical temperatures separating the low and high temperature behavior of the resistivity are Debye temperature  $T_D = \hbar v_s q_D / k_B$  for normal metals, and Bloch-Grüneisen temperature  $T_{BG} = \hbar v_s 2k_F / k_B$  for semimetals.

We expect the (phenomenological) Hamiltonian equations

$$\frac{d(\hbar\vec{k})}{dt} = -\frac{\partial E(\vec{k}, \vec{r}, t)}{\partial \vec{r}}; \quad \frac{d\vec{r}}{dt} = \frac{\partial E(\vec{k}, \vec{r}, t)}{\partial(\hbar\vec{k})}, \quad (2)$$

where  $E(\vec{k}, \vec{r}, t) \equiv E(\vec{k}, a(\vec{r}, t))$  is a band energy in terms of the local atomic spacing  $a(\vec{r}, t)$ , or better, the local strain field derived from the atomic spacings. We take the spacial dependence of  $E(\vec{k}, \vec{r}, t)$  to be proportional to the deformation potential.

*Properties and influence of the deformation potential.* In our semiclassical approach, the deformation potential generates a classical force deflecting electron ray paths. The picture is one of gently curving rays suffering the unruly time dependent forces of the deformations. From the phase and coordinate space perspective, the motion is expected to be a branched flow [7, 8, 18, 19]. Electron branched flow has already been seen, and literally imaged before, in the Westervelt lab work on 2D electron gases [8]. There the potentials were fixed in space by the uneven distribution of atoms in the donor layer. In spite of this difference, the experimental images of branched flow of electrons lend credence to the present theory.

Here, we have a smooth but time and temperature dependent branched evolution responsible for momentum diffusion and resistivity. In Fig. 2 we see contour maps of the two dimensional deformation field for two temperatures and the branched flow evolution of the same manifold of trajectories riding over the potential. The trajectories were launched from a point in space over a small range of angles as seen at the left in each panel. There are no collisions with defects, but the finite mobility is evident.

*Classical ray path tests.* Now we investigate the electron momentum diffusion numerically. The energy of electron is  $E(\vec{k}, \vec{r}, t) = E(\vec{k}) + V_D(\vec{r}, t)$ . For each temperature, we run thousands of trajectories with the same initial kinetic energy, using random initial directions and positions, and several realizations of the random deformation potential. We use  $v_s \sim 1 \times 10^4$  m/s as the speed of longitudinal acoustic phonons,  $a \sim 10^{-10}$  m and  $k_F \sim 10^8$  m<sup>-1</sup> as typical values of lattice spacing (length scale) and the Fermi wavenumber, respectively, for metals. For semimetals,  $k_F$  depends on carrier density.

The function  $c(t) = \vec{p}(0) \cdot \vec{p}(t)$  measures the correlation between the initial momentum and the momentum at a time  $t$ . In a Gaussian random diffusive process, we have  $\langle c(t) \rangle = |\vec{p}(0)|^2 e^{-\frac{t}{\tau}}$ ; we suppose for now that we can treat the deformation potential as causing Gaussian random diffusion of momentum.

The results in Fig. 3 show an approximate  $T^4$  low temperature rise in resistivity in 2D, rolling over to near  $T$

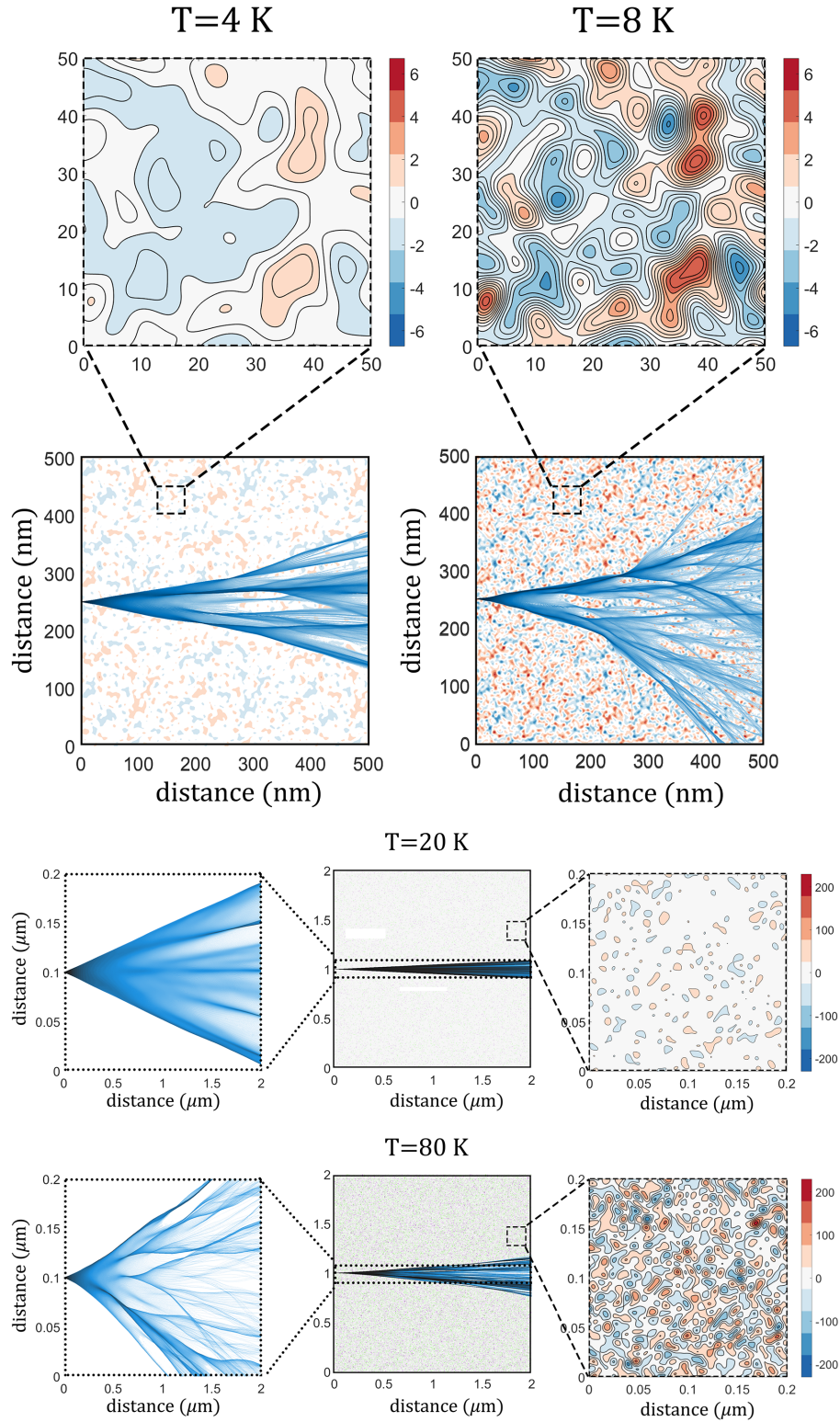


FIG. 2. In blue tones, ensembles of classical electron pathways launched uniformly over a range of angles reveal branched flow typical of weak random scattering [8, 19, 20]. In the top two rows, scales of branched flow at two temperatures for typical ordinary metals, here treated for graphical purposes as 2D. In the bottom two rows the parameters are appropriate to graphene, with much longer mean free paths. Deformation potential contours calculated with equation (1) are shown. Identical random phases were used at the two temperatures. The peaks and valleys get higher and deeper as temperature increases. Below the Bloch-Grüneisen temperature, the length scale of potential decreases in proportion to the increasing temperature. It is statistically self-similar after scaling height and distance by temperature, and is statistically the same for every metal except for scale.

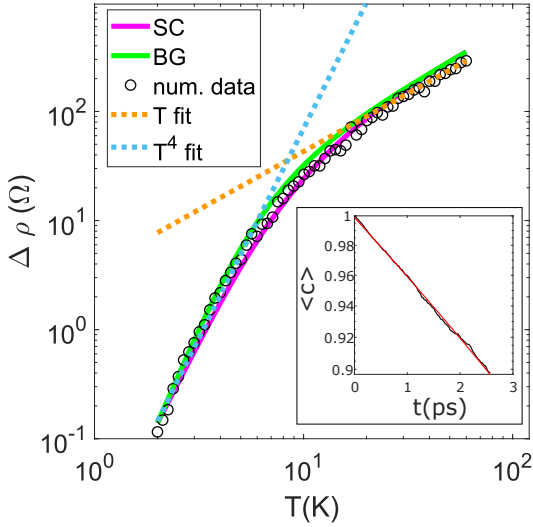


FIG. 3. In a log-log plot, the dependence of the resistivity with temperature is shown. We fitted our numerical results in 2D to the eq. 3 (SC) and eq. 4 (BG) by adjusting the temperature independent prefactor. The carrier density is  $n = 5 \times 10^{12} \text{ cm}^{-2}$  and the Bloch-Grüneisen temperature  $T_{BG} = 30 \text{ K}$ . The inset shows a typical computation of the correlation as a function of time, revealing an exponential decay for the given time window. The slope of this plot is taken as the relaxation time  $\tau$  and the resistivity from electron-phonon interaction was calculated from  $\Delta\rho = \rho - \rho_0 = \frac{m}{ne^2\tau}$ ;  $m$  is the electron mass,  $\rho_0$  is the resistivity at  $T = 0 \text{ K}$ , due to impurities. We use  $\rho_0 = 0$ . A key experimental paper by Efetov and Kim [21] showed very similar plots in graphene with doping varying the carrier density almost a factor of 10.

at high temperature, in agreement with experiment[21]. The inset of Fig. 3 shows the exponential decay of the correlation for the given time window. If the initial decay is used, the result is close to  $T^4$ . For longer observation windows the power law goes closer to  $T^3$  (presumably  $T^4$  in 3D but we have not checked this).

Only for a Markovian Gaussian random process should the sampling time not matter, and our numerical results show a non-Gaussian momentum distribution for short to moderate times. The concept of a single relaxation time or mean free path may need re-examining, but this is beyond the scope of this paper. It would be surprising if exact integer power laws for temperature dependence of the resistivity emerged numerically, except in limiting approximations, as derived below.

*Classical perturbative derivation of the temperature dependence of resistivity.* For the frozen deformation potential  $V_D(\vec{r}, t) = V_D(\vec{r})$ , the momentum correlation function can be calculated analytically using classical perturbation theory. One knows  $\delta\vec{p}(t) = \vec{p}(t) - \vec{p}(0) = \int_0^t dt' \left( -\frac{\partial V_D(\vec{r}(t'))}{\partial \vec{r}(t')} \right)$ . Then,  $\vec{p}(0) \cdot \vec{p}(t) = |\vec{p}(0)| |\vec{p}(t)| \cos \chi(t) \approx |\vec{p}(0)|^2 \left( 1 - \frac{|\delta\vec{p}(t)|^2}{2|\vec{p}(0)|^2} \right)$  where  $\chi(t)$  is the angle between the two momenta, and the quasielasticity of scattering  $|\vec{p}(t)| \approx |\vec{p}(0)|$  and the law of co-

sine for angle  $\chi(t)$  were used. Take the ensemble average (average over all possible realizations of deformation potentials specified by  $\{\phi_{\vec{q}}\}$ ) to obtain  $\langle c(t) \rangle = \langle \vec{p}(0) \cdot \vec{p}(t) \rangle = |\vec{p}(0)|^2 \left( 1 - \frac{\langle |\delta\vec{p}(t)|^2 \rangle}{2|\vec{p}(0)|^2} \right)$  where  $\langle |\delta\vec{p}(t)|^2 \rangle =$

$$\mathbb{E}_d^2 \sum_{|\vec{q}| < q_{max}} \frac{2\hbar q}{\rho_m V v_s} \left( \frac{\vec{q} \cdot \vec{p}(0)/m}{q \cdot \vec{p}(0)/m} \right)^2 \frac{1 - \cos(\vec{q} \cdot \vec{p}(0)t/m)}{e^{\hbar v_s q/k_B T} - 1}$$
 using un-

perturbed trajectory  $\vec{r}^{(0)}(t') = \vec{p}(0)t'/m$ . Note sinusoidal oscillation with different phases vanishes due to the ensemble average, *i.e.*,  $\langle \cos(A + \phi_{\vec{q}}) \cos(B + \phi_{\vec{q}}) \rangle = \delta_{\vec{q}, \vec{q}'}$   $\langle \cos(A + \phi_{\vec{q}}) \cos(B + \phi_{\vec{q}}) \rangle = \delta_{\vec{q}, \vec{q}'}$ .

For 2D, we use polar coordinate for  $\vec{q}$  where angle  $\theta$  is chosen such that  $\vec{q} \cdot \vec{p}(0) = q|\vec{p}(0)| \sin \theta$ , and use  $|\vec{p}(0)| = mv_F$ , then

$$\begin{aligned} \langle |\delta\vec{p}(t)|^2 \rangle &= \mathbb{E}_d^2 \int_0^{q_{max}} \frac{dq q}{(2\pi/L)^2} \int_0^{2\pi} d\theta \frac{2\hbar q}{\rho_m V v_s} \left( \frac{1}{v_F \sin \theta} \right)^2 \\ &\quad \times \frac{1 - \cos(qv_F t \sin \theta)}{e^{\hbar v_s q/k_B T} - 1} \\ &= \mathbb{E}_d^2 \int_0^{q_{max}} \frac{dq q}{(2\pi)^2} \frac{2\hbar q}{\rho_m v_s} \frac{1}{v_F^2} \frac{f(qv_F t)}{e^{\hbar v_s q/k_B T} - 1} \end{aligned}$$

where  $f(A) = A\pi \{ J_1(A)[-2 + A\pi H_0(A)] + AJ_0(A)[2 - \pi H_1(A)] \}$  and  $H$ 's and  $J$ 's are Struve and Bessel functions, respectively. Looking at sufficiently long time correlation such that  $A = qv_F t \gg 1$  holds, one can approximate  $f(A) \approx 2\pi A$ . Then, one can obtain momentum relaxation time  $\tau$  from  $\langle c(t) \rangle = |\vec{p}(0)|^2 (1 - t/\tau)$ , and get semiclassical (SC) resistivity  $\Delta\rho_{SC}(T) = \frac{m}{ne^2\tau}$  in 2D

$$\Delta\rho_{SC}(T) = \frac{m}{ne^2} \frac{1}{2|\vec{p}(0)|^2} \mathbb{E}_d^2 \int_0^{q_{max}} \frac{dq q}{(2\pi)^2} \frac{2\hbar q}{\rho_m v_s v_F^2} \frac{2\pi q v_F}{e^{\hbar v_s q/k_B T} - 1}$$

The factor of  $q^3$  has three origins: First there is  $q$  for the growth of density of states; another  $q$  arises from the square of the  $(\sqrt{\omega_q})^2 = v_s q$  in the numerator of equation (1), and finally we just discussed another factor of  $q$  coming from the ensemble and angular average with long time correlation.

For specificity, one can look at graphene where  $k_F^2 = \pi n$ ,  $|\vec{p}(0)| = mv_F = \hbar k_F$ ,  $q_{max} = 2k_F$  and substitute (renormalized wavenumber)  $x = q/q_{max}$ , (renormalized inverse temperature)  $z = T_{BG}/T$  to obtain

$$\Delta\rho_{SC}(T) = \frac{8\mathbb{E}_d^2 k_F}{e^2 \rho_m v_s v_F^2} \int_0^1 dx \frac{x^3}{e^{zx} - 1} \quad (3)$$

This is comparable to the generalized Bloch-Grüneisen (BG) formula [21, 22]

$$\Delta\rho_{BG}(T) = \frac{8\mathbb{E}_d^2 k_F}{e^2 \rho_m v_s v_F^2} \int_0^1 dx \frac{zx^4 \sqrt{1-x^2}}{(1-e^{-zx})(e^{zx}-1)} \quad (4)$$

where the factor  $\sqrt{1-x^2}$  originates from the chiral nature of the carriers in graphene and shows the absence of backscattering for the carriers.

Likewise, in 3D metal where  $n = \frac{k_F^3}{3\pi^2}$  and  $q_{max} = q_D$ , there is an extra factor of  $q$  in the density of states, so

one obtains

$$\Delta\rho_{SC}(T) = \frac{3\pi\mathbb{E}_d^2 q_D^5}{4k_F^4 e^2 \rho_m v_s v_F^2} \int_0^1 dx \frac{x^4}{e^{zx} - 1} \quad (5)$$

This compares with the Bloch-Grüneisen formula [2]

$$\Delta\rho_{BG}(T) = \frac{3\pi\mathbb{E}_d^2 q_D^5}{4k_F^4 e^2 \rho_m v_s v_F^2} \int_0^1 dx \frac{zx^5}{(1 - e^{-zx})(e^{zx} - 1)} \quad (6)$$

It should be noted both SC and BG ((3) and (4) in 2D and (5) and (6) in 3D) give correct temperature dependence  $\sim T^4$  in 2D and  $\sim T^5$  in 3D for low temperature and  $\sim T$  for high temperature. In fact, the SC and BG results differ only by a factor of order one for all temperature ranges.

This difference originates from the factor  $\frac{zx}{1 - e^{-zx}}$  in (4) and (6) that comes in when one considers Fermi statistics of electrons in the scattering processes from occupied to unoccupied states. For high temperature limit  $z \rightarrow 0$ , the factor becomes unity,  $\frac{zx}{1 - e^{-zx}} \rightarrow 1$ . Thus, if one ignores the Fermi statistics of the electrons by using the high-temperature Fermi distribution for all temperatures, and only considers the Bose-Einstein distribution of phonons, the BG results (4) and (6) reduce to the SC results (3) and (5) (apart from the graphene-specific factor  $\sqrt{1 - x^2}$  in 2D). This implies the reverse—if Fermi statistics of electrons are incorporated in our SC model, the BG result will be obtained—is likely to be true.

*Going beyond the classical perturbation theory.* There is a correlation between successive scattering events: the forces on a trajectory from the deformation potential self-average, nearly vanishes over straight paths. Pushes one way are followed by opposing pushes; this is not a simple random walk in momentum. Actual classical ray paths are not perfectly straight and the averaging to zero is not complete. However, the averaging encourages nearly linear trajectories, which feeds more averaging. This will perhaps lead to interesting nonlinear behavior as a function of the potential strength. The consequences are already present in our numerical studies but ignored in the analytical derivation.

For example, the resistivity going exactly as  $T$  at high temperature is in question, since although the classical perturbation theory gives that power, there are known corrections provided by the nonlinear trajectories. Indeed the experimental rise is typically more like  $T^{1.2}$ , a significant deviation (see Table 2.1 of Kasap [23]).

*Thermal relaxation and fluctuation.* Energy is exchanged between electrons and phonons in our model because electrons collide quasielastically with moving deformation hills and valleys. We ignore the back-reaction on the heavy lumbering deformations, but the nimble electrons come off a collisions going a little faster or slower.

It is neither possible nor necessary to keep track of individual phonons.

The semiclassical quasielastic approach comes with a mechanism for thermalization, although we have not yet explored this numerically. There are delicate questions of screening and charge neutrality to be faced, as it was in the case of ultrasound attenuation[] The relaxation time for momentum and energy is the same, so the Wiedemann-Franz law should follow without the usual free electron model and unspecified relaxation mechanism.

*Conclusion.* We have given a non-perturbative semiclassical and quantitatively successful theory of the temperature dependence of electrical resistivity in metals and semimetals, treating the deformation potential as a classical field. The approach suggests a new model of electron-phonon interactions, involving quasielastic collisions of electrons with slowly moving (as seen by the electrons) deformation potential hills and valleys. When we make classical perturbation theory approximations to our expressions, we find the Bloch-Grüneisen  $T^4$  temperature dependence in 2D and  $T^5$  in 3D, including prefactors that differ by a factor of order one, as limiting low temperature behaviors. An approximate, not exact,  $T^4$  low temperature rise in resistivity in 2D also appeared numerically, and there are reasons to believe the temperature rise need not be analytic. The perfect agreement between the traditional one phonon inelastic perturbative approach and the semiclassical nonperturbative approach in the weak field limit should hold, if both approaches are valid in that limit. The two very different approaches thus validate each other.

The semiclassical approach presented here can however be taken into the strong field limit, appropriate to large deformation potentials and/or high temperatures. There is a smorgasbord of cases and phenomena to study, including metals that rise with a power higher than 1 above their Debye temperatures, and the mystifying “speed limit” of metals and strange metals [24].

The model of electron-phonon interactions has been expanded from one phonon inelastic events to smooth quasielastic ones, accounting for both energy and momentum changes with the same forces.

*Acknowledgements.* We thank Profs. Efthimios Kaxiras, Philip Kim, Peter Milonni, and Bertrand Halperin for stimulating and informative discussions surrounding the issues raised in this paper. Chris Fechisin was very helpful concerning the thermal coherent state ensemble, and Elizabeth Koslov with issues of dynamics on the deformation potential. We thank the NSF the Center for Integrated Quantum Materials (CIQM) Grant No. DMR-12313 19, and NSF CHE 1800101, and acknowledge the support of Real Colegio Complutense (RCC) through the Faculty Research Fellowship that supported the research of Alvar Daza at the Harvard Faculty of Arts and Sciences.

- 
- [1] J. Bardeen and W. Shockley, *Phys. Rev.* **80**, 72 (1950).
- [2] J. Ziman, *Electrons and Phonons: The Theory of Transport Phenomena in Solids*, International series of monographs on physics (OUP Oxford, 2001).
- [3] E. H. Hwang and S. Das Sarma, *Phys. Rev. B* **79**, 165404 (2009).
- [4] N. Ashcroft and N. Mermin, *Solid State Physics*, HRW international editions (Holt, Rinehart and Winston, 1976).
- [5] A. B. Pippard, *Proceedings of the Royal Society of London. Series A, Mathematical and Physical Sciences* **257**, 165 (1960).
- [6] M. H. Cohen, M. J. Harrison, and W. A. Harrison, *Phys. Rev.* **117**, 937 (1960).
- [7] A. Patsyk, U. Sivan, M. Segev, and M. A. Bandres, *Nature* **583**, 60 (2020).
- [8] M. Topinka, B. LeRoy, R. Westervelt, S. Shaw, R. Fleischmann, E. Heller, K. Maranowski, and A. Gossard, *Nature* **410**, 183 (2001).
- [9] H. Degueldre, J. J. Metzger, T. Geisel, and R. Fleischmann, *Nature Physics* **12**, 259 (2016).
- [10] M. Sargent, M. O. M. O. Scully, and W. E. W. E. Lamb, *Laser physics* (London : Addison-Wesley, 1974) includes bibliographical references.
- [11] E. J. Heller and D. Kim, *The Journal of Physical Chemistry A* **123**, 4379 (2019), pMID: 30892041, <https://doi.org/10.1021/acs.jpca.8b11746>.
- [12] E. Schrodinger, *Naturwiss.* **14**, 664 (1926).
- [13] C. Kittel, *Introduction to Solid State Physics* (John Wiley & Sons, Inc., New York, 1986).
- [14] I. M. Lifshitz and A. M. Kosevich, *Sov. Phys. JETP* **2**, 646 (1956).
- [15] G. D. Mahan, *Many-Particle Physics* (Plenum, New York, 1993).
- [16] M. Lax, *Rev. Mod. Phys.* **23**, 287 (1951).
- [17] M. S. Fuhrer, *Physics* **3** (2010), 10.1103/Physics.3.106.
- [18] E. J. Heller, L. Kaplan, and A. Dahlen, *Journal of Geophysical Research: Oceans* **113** (2008).
- [19] J. J. Metzger, R. Fleischmann, and T. Geisel, *Phys. Rev. Lett.* **105**, 020601 (2010).
- [20] E. Heller, L. Kaplan, and A. Dahlen, *Journal of Geophysical Research: Oceans* **113** (2008).
- [21] D. K. Efetov and P. Kim, *Phys. Rev. Lett.* **105**, 256805 (2010).
- [22] E. H. Hwang and S. Das Sarma, *Phys. Rev. B* **77**, 115449 (2008).
- [23] S. Kasap and P. Capper, *Springer handbook of electronic and photonic materials* (Springer, 2017).
- [24] J. Zaanen, *Nature* **430**, 512 (2004).